厚生労働科学研究費補助金（化学物質リスク研究事業）
「抗原性物質への免疫応答に対するナノマテリアル経皮曝露の影響に関する
評価手法の開発研究」
分担研究報告書（平成 26 年度）

ナノマテリアルのアジュバント活性に関する貪食細胞を用いた in vitro 評価手法の開発研究

分担研究者：　最上　知子　国立医薬品食品衛生研究所　生化学部　部長
研究協力者：　崔　紅艶　　国立医薬品食品衛生研究所　生化学部　派遣研究員

研究要旨

本研究では in vitro でのアジュバント活性評価系を確立し、酸化チタン等のナノマテリアルの活性を評価することを目的として検討を行った。抗原免疫時のアジュバント作用には、サイトカイン IL-1β 産生を誘導する NLRP3 インフラマソームが決定的な役割を持つことが報告されている。そこで、アジュバント活性の in vitro 評価手法として、NLRP3 インフラマソーム活性化に着目し検討を行った。マクロファージ系培養細胞である PMA 分化 THP-1 細胞を用い、NLRP3 の siRNA ノックダウン及び caspase-1 阻害剤を利用し、NLRP3 インフラマソーム依存的な IL-1β 産生応答を測定できる系を確立した。三種類の酸化チタンナノマテリアルについて検討を行い、アジュバントとして汎用されている酸化アルミニウムゲル（Alum）の場合と同様に、濃度依存的な活性を有することを明らかにした。また貪食阻害剤を用い、酸化チタンの粒子径が小さい場合には、貪食によらない直接の活性化を示唆する知見を得た。

A. 研究目的

抗原免疫時のアジュバント作用においては、貪食細胞による貪食・インフラマソームの活性化・炎症性サイトカイン産生が重要であることが明らかにされている。とりわけ、成熟型 IL-1β の産生をもたらす NLRP3 インフラマソーム・caspase-1 の活性化が決定的な役割を持っており、NLRP3 や caspase-1 ノックアウトマウスにおいては、水酸化アルミニウム（Alum）のアジュバント活性が失われることが報告されている。Alum はヒトや動物に使用するワクチンに広く使用されているアジュバントである。

我々はこれまでにマクロファージが多層カーボンナノチューブ MWCNT を貪食し、NLRP3 活性化を介して IL-1β を産生することを報告しており、酸化チタン等のナノマテリアルについても同様のアジュバント様作用により抗原感作を促進する可能性が懸念される。

本研究班では、酸化チタン、酸化亜鉛等の経皮暴露が抗原タンパク質の経皮感作に及ぼす影響について in vivo 及び in vitro での評価系開発を目的としている。本分担研究においては、貪食細胞を用いた in vitro アジュバント活性評価法の検討を行う。

B．研究方法

1．実験材料および試薬

被検物質としては、下記の 3 種類の酸化チタンナノマテリアル（表面未処理）を用いた。

酸化チタン A（粒子径：15 nm）

酸化チタンB（粒子径：35 nm）
酸化チタンC（粒子径：6 nm）

陽性対照とした多層カーボンナノチューブは、MWCNT-SD1（長さ8 μm, 径150 nm）である。サイトカイン測定はミリポア社のMILLIPLEX™ MAPアッセイキットを用いて行った。また酸化アルミニウムゲルAlum（免疫グレードアジュバント用）はコスモバイオ株式会社より購入した。Stealth™ Select RNAi（NLRP3）およびStealth RNAi negative controlはInvitrogen社から購入した。

2．MWCNTおよびHTCFNWの分散

MWCNT- SD1は0.5%Tween 20を含むPBSに5 mg/mLの濃度で懸濁し、1～5分間バス型超音波発生装置での処理、ピペッティング、25Gシリンジ通過により分散した。酸化チタンはPBSに50mg/mLの濃度に懸濁し、3-4分間バス型超音波発生装置での処理・vortexを3回繰り返し、ピペッティング、25Gシリンジ通過により分散した。Alumは0.9%NaCl溶液に20mg/mLに懸濁された製品を解凍後vortexし使用した。

3．マクロファージ系細胞からのサイトカイン放出の測定

ヒト単球由来THP-1細胞は24wellプレートに播種し、0.3μM PMAと10%FCSを含むRPM1培地中で72時間培養してマクロファージ様に分化した。さらにPMAを除いた培地中で24時間培養したのちに、各種阻害剤あるいは溶剤で30分前処理し、引き続き上記の酸化チタン、Alum、分散MWCNTあるいは対照となる溶剤を培地に添加し各種阻害剤の存在下・非存在下で6時間培養した。培養上清を回収し、MILLIPLEX™MAPアッセイを用いてサイトカイン濃度の測定を行った。

4．siRNAを用いたNLRP3のノックダウン

THP-1細胞を72時間PMAでマクロファージ様に分化したのち、Stealth™ Select RNAi（NLRP3, sense2およびantisense2）あるいはStealth RNAi negative controlをlipofectamine RNAi MAX試薬(Invitrogen)を用いて細胞に導入し、24時間後に酸化チタンならびにAlumに6時間曝露した。培養上清を回収し、サイトカイン濃度の測定を行った。

5．RNA抽出および定量的リアルタイムRT-PCR

NLRP3ノックダウンはmRNAを定量して評価した。細胞からRNAをRNeasy Mini Kitを用いて抽出しDNAse処理を行った。QuantiTect Probe RT-PCR Kit（Qiagen）を用いABI Prism 7300において定量的リアルタイムRT-PCRにより測定した。発現量データは18S rRNAの量で補正した。

C.研究結果

抗原免疫時のアジュバント作用には、炎症性サイトカインIL-1β産生をもたらすNLRP3インフラマソーム活性化が決定的な役割を持つことが報告されている。そこでナノマテリアルのアジュバント活性をin vitroで評価する方法として、マクロファージ系培養細胞を用いてNLRP3インフラマソーム活性化を介するIL-1β産生の促進を測定する方法を検討した。

1．酸化チタンナノマテリアルはAlumと同様にマクロファージ系細胞からのIL-1β産生を促進する

PMA分化THP-1細胞を用い、汎用されているアジュバントAlumを用いて検討したところ、濃度（50～250 μg/mL）に依存し、IL-1β産生を促進することを確認した。同様に、三種類の酸化チタンナノマテリアル（A～C）がいずれも濃度依存的（50～250 μg/mL）にIL-1β産生を促進することを見いだした（図1）。

2．酸化チタンナノマテリアルはNLRP3-caspase-1を介してIL-1β産生を促進する

酸化チタンナノマテリアル（A～C）ならびに

Alum による IL-1β産生の促進は、caspase-1 阻害剤である z-YVAD-fmk によりほぼ完全に抑制された（図 2A）。また、細胞の NLRP3 を特異的 siRNA で処理し、NLRP3 の mRNA レベルを約 15%までノックダウンした場合においても（図 2B）、Alum による IL-1β産生促進は約 90%、酸化チタンナノマテリアルによる IL-1β産生も約 90～100%抑制された（図 2C）。

3. 酸化チタンナノマテリアルによる IL-1β産生促進に対する貪食阻害剤の影響は粒子により異なる

IL-1β産生促進作用に対する貪食阻害剤 cytochalacin D（Cyt D）の影響はナノマテリアルによって異なっていた。細胞を 0.2μM の Cyt D で処理すると、多層カーボンナノチューブ MWCNT-SD1 による IL-1β産生は、ほぼ完全に抑制されたのに対し、酸化チタンナノマテリアル（A～C）による IL-1β産生は逆に 30～50%促進された（図 3）。Alum による促進は約 50%抑制された。Cyt D 濃度を 1μM に上昇させた場合には、酸化チタン A および B は 60～50%抑制されたが、酸化チタン C の抑制はわずかであり、貪食阻害剤の効果は粒子により異なった。Alum による IL-1β産生誘導は、高濃度ではほぼ完全に抑制された。

D. 考察

本研究課題は、ナノマテリアルが感作の際のアジュバントとなる可能性、すなわちナノマテリアルの経皮曝露が抗原感作性を増強する可能性について検討するものである。この分担課題においては、in vitro でのアジュバント活性評価系を確立するとともに、酸化チタンナノマテリアルの活性評価を行った。

抗原免疫時のアジュバント作用では、炎症性サイトカイン IL-1β産生を誘導する NLRP3 インフラマソームが決定的な役割を果たしており、例えば Alum のアジュバント作用は NLRP3 や caspase-1 のノックアウトマウスでは消失することが報告されている。NLRP3 はインフラマソームと呼ばれるタンパク複合体を形成し、内外の危険分子シグナルを受容して caspase-1 を活性化し、caspase-1 は IL-1β を前駆体から切断して活性化する役割を持つことが知られている。

そこでナノマテリアルのアジュバント活性の in vitro 評価手法として、NLRP3 インフラマソーム活性化に着目し、マクロファージ系培養細胞を用いて評価する方法を検討した。PMA 分化 THP-1 細胞において NLRP3 の siRNA ノックダウンならびに caspase-1 阻害剤を利用し、アジュバントとして汎用される Alum が貪食され、NLRP3 および caspase-1 依存的に IL-1β を産生する応答を測定できる系を確立した。

この系を用い、3 種類の酸化チタンナノマテリアル A～C はいずれも、濃度に応じ NLRP3 依存的に IL-1β産生を促進することを明らかにした。しかし、貪食阻害剤の影響は粒子によって異なり、サイズが小さい酸化チタン C は貪食されずに細胞膜を透過し NLRP3 インフラマソームを活性化することが示唆された。小さな粒子は経皮暴露において表皮細胞のインフラマソームを直接活性化する可能性が考えられることから、平成 27 年度に検討を予定している。

E. 結論

アジュバント活性の in vitro 評価手法として、マクロファージ系培養細胞を用いた NLRP3 インフラマソーム活性化のアッセイ系を確立した。酸化チタン粒子が濃度依存的な活性を有することが判明し、粒子径が小さい場合は貪食によらない直接の活性化が示唆された。

F. 研究発表

1. 学会発表

1. Cui H, Wu W, Okuhira K, Miyazawa K, Hattori T, Sai K, Naito M, Suzuki K, Nishimura T, Sakamoto Y, Ogata A, Maeno T, Inomata A, Nakae D, Hirose A, Nishimaki-Mogami T. High-temperature calcined fullerene nanowhiskers as well as

long needle-like multi-wall carbon nanotubes have abilities to induce NLRP3-mediated IL-1beta secretion. *Biochem Biophy Res Commun*, 452 : 593-599. (2014)

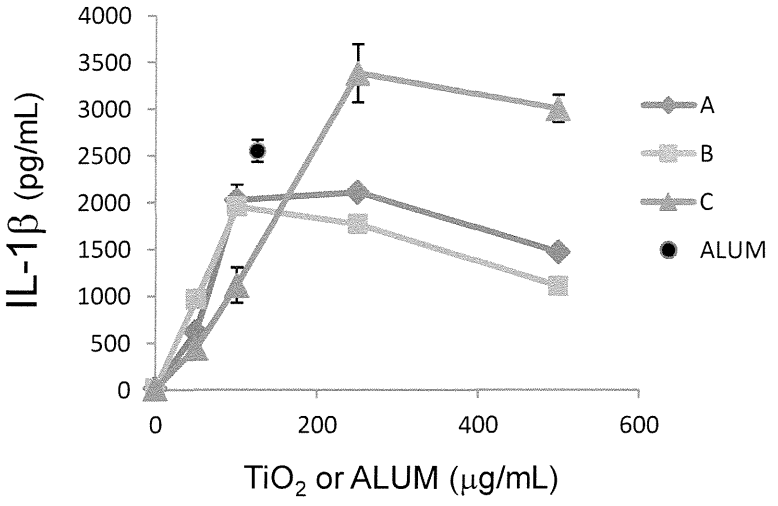

図1. 酸化チタンナノマテリアル(A,B,C)ならびにALUMはTHP-1マクロファージからのIL-1βの分泌を促進する

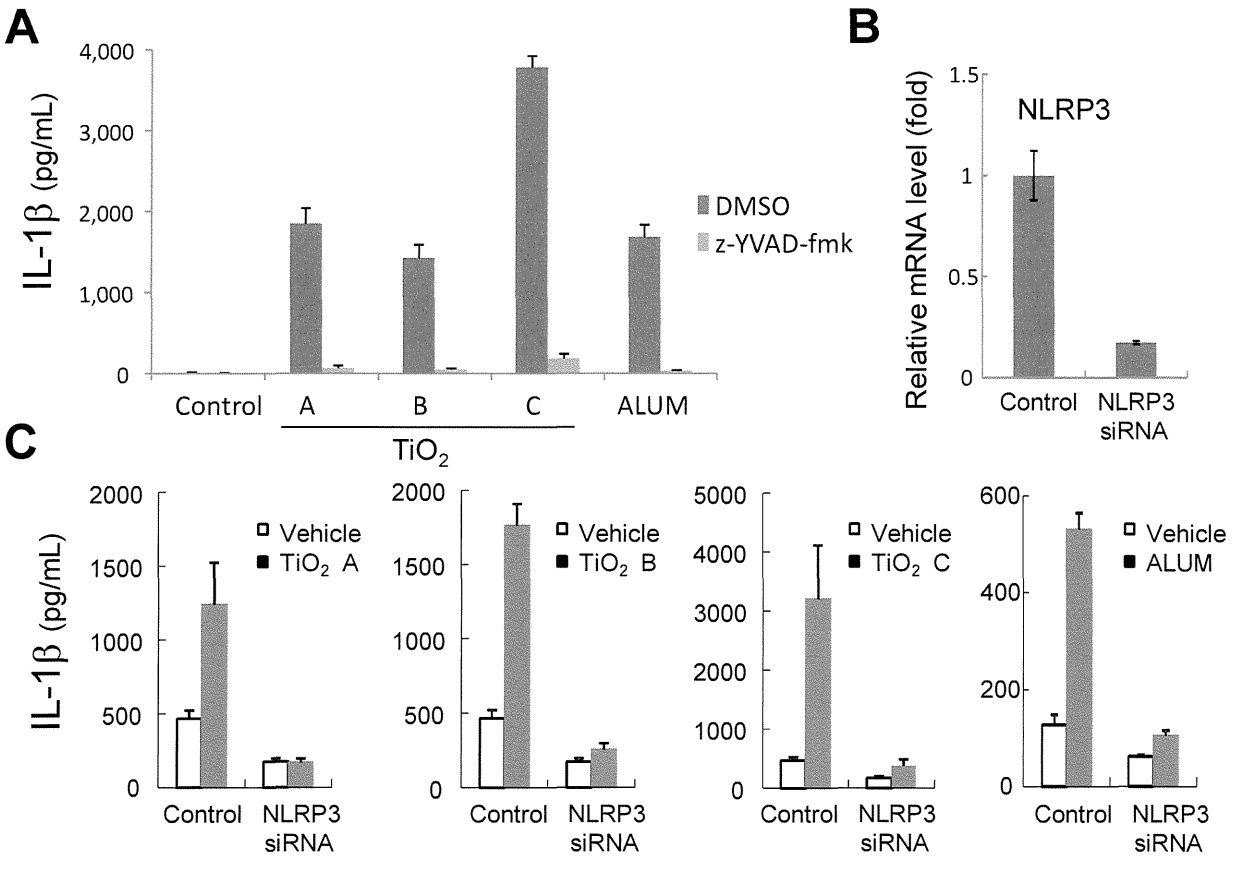

図2. 酸化チタンナノマテリアルならびにALUMによるTHP-1マクロファージからのIL-1β分泌促進は、caspase-1阻害剤処理(A)あるいはNLRP3のsiRNAノックダウン(C)により抑制される. ノックダウンは mRNAレベル(B)を測定して評価した.

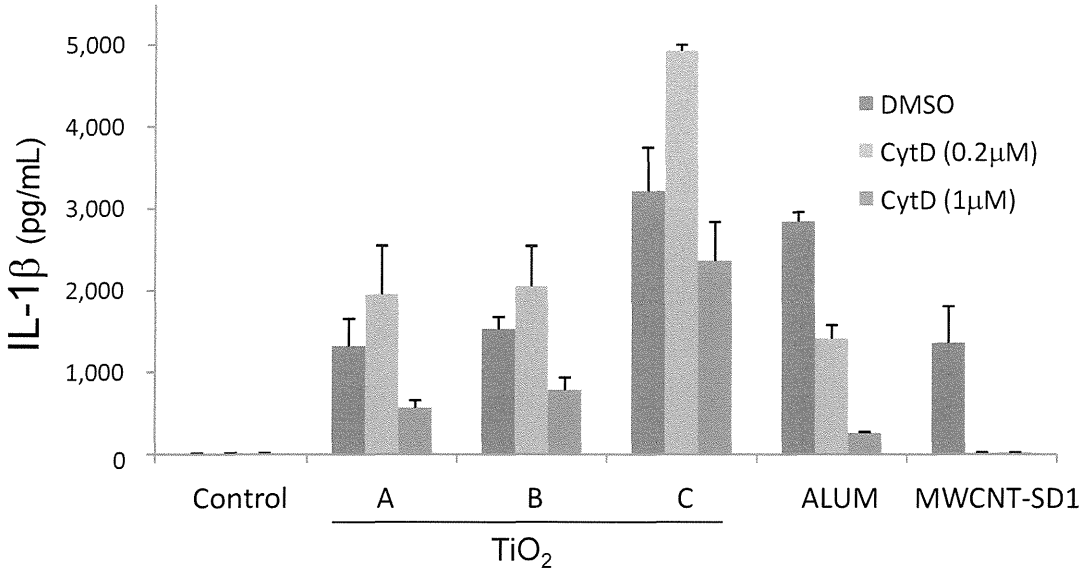

図3. 酸化チタンナノマテリアルによるTHP-1マクロファージからのIL-1β分泌誘導は、MWCNTによるIL-1β分泌誘導とは異なり、貪食阻害剤(cytochalasin D) による抑制を受けにくい

Ⅲ．研究成果の刊行に関する一覧表

研究成果の刊行に関する一覧表

雑誌

発表者氏名	論文タイトル名	発表誌名	巻号	ページ	出版年
Cui H, Wu W, Okuhira K, Miyazawa K, Hattori T, Sai K, Naito M, Suzuki K, Nishimura T, Sakamoto Y, Ogata A, Maeno T, Inomata A, Nakae D, Hirose A, Nishimaki-Mogami T.	High-temperature calcined fullerene nanowhiskers as well as long needle-like multi-wall carbon nanotubes have abilities to induce NLRP3-mediated IL-1beta secretion.	*Biochem Biophy Res Commun*,	452	593-599	2014

IV. 研究成果の刊行物・別刷

Biochemical and Biophysical Research Communications 452 (2014) 593–599

Contents lists available at ScienceDirect

Biochemical and Biophysical Research Communications

journal homepage: www.elsevier.com/locate/ybbrc

High-temperature calcined fullerene nanowhiskers as well as long needle-like multi-wall carbon nanotubes have abilities to induce NLRP3-mediated IL-1β secretion

Hongyan Cui [a], Weijia Wu [a], Keiichiro Okuhira [a], Kun'ichi Miyazawa [b], Takayuki Hattori [a], Kimie Sai [a], Mikihiko Naito [a], Kazuhiro Suzuki [a], Tetsuji Nishimura [a], Yoshimitsu Sakamoto [c], Akio Ogata [c], Tomokazu Maeno [c], Akiko Inomata [c], Dai Nakae [c], Akihiko Hirose [a], Tomoko Nishimaki-Mogami [a,*]

[a] Division of Biochemistry and Metabolism, Division of Biochemistry and Molecular Biology, Division of Environmental Chemistry, Division of Risk Assessment, and Biological Safety Research Center, National Institute of Health Sciences, Tokyo 158-8501, Japan
[b] Fullerene Engineering Group, Materials Processing Unit, National Institute for Materials Science, Tsukuba, Ibaraki 305-0044, Japan
[c] Department of Environmental Health and Toxicology, Tokyo Metropolitan Institute of Public Health, Tokyo 169-0073, Japan

ARTICLE INFO

Article history:
Received 4 August 2014
Available online 30 August 2014

Keywords:
Carbon nanotubes
Fullerene nanowhiskers
IL-1β
NLRP3

ABSTRACT

Because multi-wall carbon nanotubes (MWCNTs) have asbestos-like shape and size, concerns about their pathogenicity have been raised. Contaminated metals of MWCNTs may also be responsible for their toxicity. In this study, we employed high-temperature calcined fullerene nanowhiskers (HTCFNWs), which are needle-like nanofibers composed of amorphous carbon having similar sizes to MWCNTs but neither metal impurities nor tubular structures, and investigated their ability to induce production a major pro-inflammatory cytokine IL-1β via the Nod-like receptor pyrin domain containing 3 (NLRP3)-containing flammasome-mediated mechanism. When exposed to THP-1 macrophages, long-HTCFNW exhibited robust IL-1β production as long and needle-like MWCNTs did, but short-HTCFNW caused very small effect. IL-1β release induced by long-HTCFNW as well as by long, needle-like MWCNTs was abolished by a caspase-1 inhibitor or siRNA-knockdown of NLRP3, indicating that NLRP3-inflammasome-mediated IL-1β production by these carbon nanofibers. Our findings indicate that the needle-like shape and length, but neither metal impurities nor tubular structures of MWCNTs were critical to robust NLRP3 activation.

1. Introduction

Carbon nanotubes (CNTs) are increasingly being used in various industrial fields because of their unique electronic and mechanical properties. However, these unique physicochemical properties, especially the asbestos-like shape and size with a high-aspect ratio, are currently of great concern with respect to the environment and human health [1]. A variety of multiwall carbon nanotubes (MWCNTs) and single-wall carbon nanotubes have been produced, and some of these materials have been shown to cause mesothelioma after injection into the abdominal cavities of p53+/− mice [2] or the scrotum of wild-type rats [3]. Inflammatory cell recruitment and granulomas [4] and elevated mRNA expression of pro-inflammatory cytokines and chemokines in peritoneal cells [5] were induced by MWCNTs injected into the abdominal cavities of mice. Pulmonary exposed MWCNTs were shown to reach subpleural tissue and macrophages in mice and rats and to induce fibrosis, inflammation, allergic immune responses [6–8] and mesothelial proliferation [9]. Abundant inflammatory cell infiltration and increased pro-inflammatory cytokine levels in the pleural cavity were also observed [9,10].

IL-1β is an important proinflammatory cytokine that is generated at sites of injury, infection, or immunological challenge to recruit immune cells [11]. It is very likely that IL-1β plays a major role in MWCNT-induced inflammation or immune responses. Recent studies have revealed that IL-1β maturation and release are controlled by a large multiprotein complex, called the inflammasome [11]. In particular, the inflammasome containing the Nod-like receptor (NLR)-family protein 3, NLRP3, can be activated

Abbreviations: MWCNTs, multi-wall carbon nanotubes; HTCFNWs, high-temperature calcined fullerene nanowhiskers; NLRP3, Nod-like receptor pyrin domain containing 3; CNTs, carbon nanotubes; SSC, side scatter; FSC, forward scatter.

* Corresponding author. Address: Division of Biochemistry and Metabolism, National Institute of Health Sciences, Kamiyoga 1-18-1, Setagaya-ku, Tokyo 158-8501, Japan. Fax: +81 3 3707 6950.
E-mail address: mogami@nihs.go.jp (T. Nishimaki-Mogami).

http://dx.doi.org/10.1016/j.bbrc.2014.08.118
0006-291X/

by a variety of danger signals or phagocytosed crystals and aggregated proteins and has been implicated in several chronic inflammatory diseases [11,12]. Certain MWCNTs have been shown to induce NLRP3-mediated IL-1β secretion [13,14]. Various MWCNTs with different physicochemical properties, including length, diameter, and contaminant metals, are produced. However, factors that are critical to inducing NLRP3 activation and/or IL-1β production remain unclear.

Shape and size of MWCNTs similar to asbestos have been implicated in their toxicity. In addition, several studies have suggested that metal contamination, which is derived from catalysts used in the synthesis of CNTs, is responsible for cytotoxicity and genotoxicity of MWCNTs [15–18] and for the redox-dependent response of macrophages [19], although this suggestion remains controversial [4,20].

In this study, we employed high-temperature calcined fullerene nanowhiskers (HTCFNWs), which are amorphous carbon nanofibers and have a needle-like morphology with similar length to MWCNTs [21]. Notably, HTCFNWs do not contain metal impurities, because they are produced from fullerene nanowhiskers by heating in vacuum [21]. Fullerene nanowhiskers are thin, single crystal nanofibers composed of C_{60} fullerene molecules that are bound via van der Waals forces [22]. We investigated the ability of long or short HTCFNW, which did not contain tubular structures and metal impurities, and various MWCNTs with different physical properties to induce IL-1β secretion, and sought to identify factors required for inducing NLRP3-mediated IL-1β release.

2. Materials and methods

2.1. Materials

We used three types of MWCNT grown in the vapor phase (Fig. 1A): MWCNT-M was provided by Nanocarbon Technologies Co., Ltd. (Tokyo, Japan). MWCNT-SD1 and MWCNT-SD2 were by Showa-Denko Co., Ltd. (Tokyo, Japan). HTCFNW-L and -S were prepared by heating fullerene nanowhiskers at 900 °C in vacuum [21]. Fullerene nanowhiskers were synthesized from C_{60} fullerene by a liquid–liquid interfacial precipitation method [23]. The size distribution of MWCNTs and HTCFNWs was determined by scanning electron microscopy. Fe contents were determined by a collision type inductively coupled plasma mass spectrometer as described [2].

2.2. Preparation of MWCNT and HTCFNW dispersions

MWCNTs were suspended in phosphate-buffered saline (PBS) containing 0.5% Tween-20 (or Tween-80) at a concentration of 0.5 mg/mL, sonicated with a bath-type sonicator (BRNSON 1200) for 1 min × 3, and then diluted with PBS to a concentration of 0.2 mg/mL. The suspension of carbon nanotubes was homogenized by passing through a 30G needle. HTCFNWs (0.5 mg/mL) were dispersed in 0.1% Tween 80.

2.3. Cell culture and treatment of cells with HTCFNWs and MWCNTs

THP-1 cells (obtained from American Type Culture Collection (ATCC), Manassas, VA) were maintained in RPM-1 medium containing 10% fetal bovine serum (FBS). Cells were plated at a density of 3.5×10^5 cells in 24 well plates, differentiated for 72 h with 0.3 μM PMA, and further incubated for 24 h without PMA. The cells were treated for 6 h with carbon nanomaterials or the indicated stimuli. As indicated, 10 μM of caspase-1 inhibitor z-YVAD-fmk (Calbiochem), 0.2 μM cytochalasin D (Sigma), 130 mM KCl, 3 mM ATP, or 3.4 μM nigericin (Sigma) was added to the incubation medium. Cell extract and the medium supernatant were collected for analysis of their cytokine content. Cell viability was assessed by release of LDH to the medium (with a Cytotoxicity Detection Kit Plus (Roche)) or by the Tetracolor one cell proliferation assay, which detects vital mitochondrial function (Seikagaku Kogyo Ltd., Tokyo).

2.4. Analysis of IL-1β secretion

IL-1β in the medium supernatant was analyzed by the Milliplex immunoassay (Merck Co., Ltd.) according to the manufacturer's protocol or by Western blotting.

2.5. Flow cytometry analysis to detect cellular uptake of MWCNTs and HTCFNWs

PMA-differentiated THP-1 cells were exposed to MWCNTs or HTCFNWs for 20 h. The cells were washed, trypsinized, suspended in PBS containing 10% FBS, and filtered through 100 μm nylon mesh. The uptake of carbon nanofibers was determined by flow cytometry (FACSCalibur™; BD Biosciences) measuring side scatter (SSC) and forward scatter (FSC) of 10,000 counts.

2.6. Western blotting

Cells were extracted with RIPA containing the protease inhibitor cocktail set III (1:100) (Calbiochem). The culture medium supernatant was concentrated with a Microkon Ultracel YM-10 (10 kDa cut-off; Millipore, Bedford, MA) or Amicon Ultra-3K (3 kDa cut-off; Millipore, Bedford, MA). Cell extract and medium samples were analyzed by polyacrylamide gel electrophoresis followed by transfer to an Immobilon-P Transfer Membrane (Millipore). Anti IL-1β antibody (sc-7884), anti-caspase-1 P-10 antibody (sc-515) (Santa Cruz Biotechnology, Inc), and anti β-actin antibody (Sigma) were used. The immunoreactive proteins were visualized using ECL (GE Healthcare, Piscataway, NJ) or a SuperSignal West Femto Substrate kit (Thermo Scientific, Rockford, IL), and light emission was quantified with a LAS-3000 lumino-image analyzer (Fuji, Tokyo, Japan).

2.7. NLRP3 knockdown by RNA interference

THP-1 cells were plated at a density of 1.75×10^6 cells in 12 well plates and were differentiated for 72 h with 0.3 μM PMA. Cells were transiently transfected with gene-specific StealthTM Select RNAi or Stealth RNAi negative control (Invitrogen, Carlsbad, CA) using lipofectamine RNAi MAX reagent (Invitrogen) for 24 h. The Stealth RNAi sequences used were human NLRP3 sense1 (5′-AACCCAGGCACACUCCUCCUGUAGC-3′), antisense1 (5′-GCUACAG GAGGAGUGUGCCUGGGUU-3′); sense2 (5′-UUCUGUUGCUGGCUU CCUCAGCACA-3′), antisense2 (5′-UGUGCUGAGGAAGCCAGCAACA GAA-3′); sense3 (5′-UCCUGUGCUACUCCAGUAACCCAGG-3′), and antisense3 (5′-CCUGGGUUACUGGAGUAGCACAGGA-3′).

2.8. RNA extraction and quantitative real-time RT-PCR

Total RNA was extracted with an RNeasy Mini Kit using on-column deoxyribonuclease digestion to eliminate genomic DNA contamination according to the manufacturer's instructions (Qiagen, Valencia, CA). Quantitative real-time RT-PCR was performed with an ABI Prism 7300 sequence detection system using the TaqMan one-step RT-PCR Master Mix Reagent Kit (Applied Biosystems, Foster City, CA) with TaqMan probes/primers as follows: human NLRP3, forward: 5′-TGAGCCTCAACAAACGCTACA-3′; reverse: 5′-CTTGCCGATGGCCAGAAG -3′; probe: 5′-FAM-CTGCGTCTCATCAAG GAGCACCGG-BHQ-3′. 18S rRNA (Applied Biosystems). Expression

data were normalized to 18S rRNA levels, and are presented as the fold difference between treated and untreated cells.

2.9. Statistical analysis

Data were analyzed by ANOVA followed by the Student–Newman–Keuls method. Statistical significance was established at the $P < 0.05$ level.

3. Results

3.1. HTCFNWs and various MWCNTs display different abilities to induce IL-1β production

HTCFNWs are the fullerene nanowhiskers heat-treated in vacuum at 900 °C and are composed of amorphous carbon [21]. Two types of HTCFNWs with different lengths and diameters (Fig. 1A) were examined for their ability to induce IL-1β production compared with MWCNT-SD1 in the human macrophage-like cell line THP-1 cells. As shown in Fig. 1B *left*, long HTCFNWs (HTCFNW-L) caused robust IL-1β production in a dose-dependent manner, which corresponded to ca. 30% of the MWCNT-SD1-induced stimulation at the same concentration. Short HTCFNWs (HTCFNW-S) had a very small but significant and phagocytosis-dependent effect (Fig. 1B *right*). We also investigated the ability of various MWCNTs with different physical properties (Fig. 1A) to stimulate IL-1β production. MWCNT-M, -SD1, or -SD2 dose-dependently induced IL-1β secretion into the medium (Fig. 1C). IL-1β production induced by MWCNT-M or -SD1 was almost completely inhibited by pretreating cells with the phagocytosis inhibitor cytochalasin D that impairs the actin filament assembly (Fig. 1D), indicating that the uptake of MWCNTs into cells is required for stimulation of IL-1β production.

These findings clearly show that MWCNTs with various physical properties exhibit different abilities to induce IL-1β production, and HTCFNWs without impurities exhibited a comparable effect to MWCNTs.

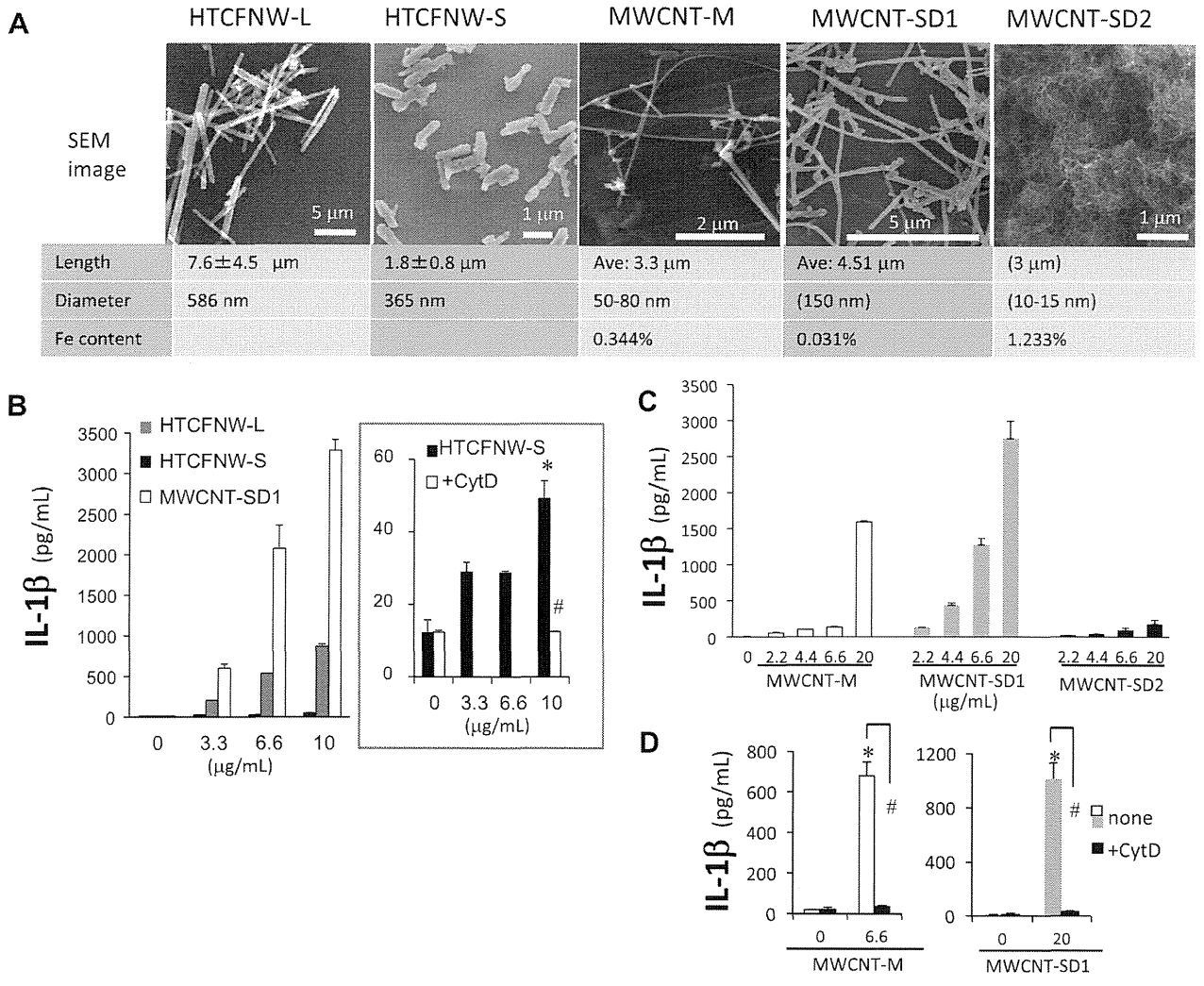

Fig. 1. HTCFNWs as well as long-, needle-like MWCNTs have abilities to induce IL-1β production. (A) Specification of the HTCFNWs and MWCNTs used in this study. Characteristics in parenthesis were provided by manufacturers. (B–D) THP-1 cells were stimulated for 6 h with the indicated amount (μg/mL of media) of HTCFNW-L, -S, and MWCNT-SD1 dispersed in Tween 80 (final concentration, 0.002%), or MWCNT-M, -SD1, and -SD2 dispersed in Tween 20 (final concentration, 0.002%) (C, D). Phagocytosis was inhibited by treating cells with cytochalasin D (0.2 μM) for 30 min before stimulation. IL-1β in the medium was analyzed by the Milliplex immunoassay. Data represent means ± S.D ($n = 2$). Significant difference from vehicle control (*) or between cytochalasin D-untreated and -treated cells (#). A vertical axis for a HTCFNW-S graph was expanded in the right panel (B).

Internalization of nanofibers by cells was evaluated with the SSC value from flow cytometry. The SSC is directly related to cell granularity and is used as a measurement of the uptake of particles or nanofibers [24,25]. Exposure of cells to MWCNT-SD1 or MWCNT-M resulted in increases in the SSC values (Fig. 2A and B), which were inhibited by the phagocytosis inhibitor cytochalasin D (Fig. 2C). MWCNT-SD2, with an agglomerate morphology, had no effect. HTCFNW-L and -S caused similar levels of SSC increase (Fig. 2D).

3.2. HTCFNW as well as MWCNTs promote caspase-1 cleavage via NLRP3 activation

The mature form of IL-1β is cleaved from the pro-IL-1β precursor by caspase-1. As shown in Fig. 3A, MWCNT-SD1 induced a potent, dose-responsive release of mature IL-1β (p17) to the medium, which was accompanied by an increase in the active caspase-1 fragment (p10). As a positive control, we confirmed that the bacterial ionophore nigericin promoted caspase-1 cleavage and IL-1β maturation. Furthermore, IL-1β secretion induced by MWCNT-M was completely inhibited by the caspase-1-inhibitor zYVAD-fmk (Fig. 3B). IL-1β release induced by MWCNT-SD1 (Fig. 3C) and HTCFNW-L (Fig. 3D) was similarly repressed by zYVAD-fmk. These findings indicate that HTCFNW-L, as well as needle-like MWCNTs, induces activation of caspase-1.

Caspase-1 is auto-activated by a signal within the multiprotein complex known as the "inflammasome" [11]. We examined whether the NLRP3-containing inflammasome is involved in MWCNT-induced IL-1β production. NLRP3 inflammasome activation is known to require potassium (K+) efflux [11]. As reported that asbestos-induced secretion of mature IL-1β was repressed by a high concentration of KCl added to the medium to inhibit K+ efflux [26], MWCNT-M-induced IL-1β secretion was blocked by KCl in the medium (Fig. 3B).

To test the role of NLRP3, siRNA knockdown of NLRP3 was performed. In THP-1 cells, three different siRNAs against NLRP3 effectively reduced NLRP3 mRNA expression (Fig. 4A). MWCNT-M-induced IL-1β secretion, determined by immunoassay, was effectively reduced by three different NLRP3 siRNAs (Fig. 4C). This reduction was accompanied by reductions of the active form of capsase-1 (p10) and cleaved IL-1β into the medium (Fig. 4B). Il-1β secretion elicited by MWCNT-SD1 or HTCFNW-L was also diminished by the NLRP3 siRNA (Fig. 4D and E). These findings clearly demonstrate that NLRP3 is involved in IL-1β maturation induced by HTCFNW-L as well as needle-like MWCNTs.

4. Discussion

In this study, we showed that fullerene-derived HTCFNWs and certain MWCNTs, with a long, needle like morphology potently

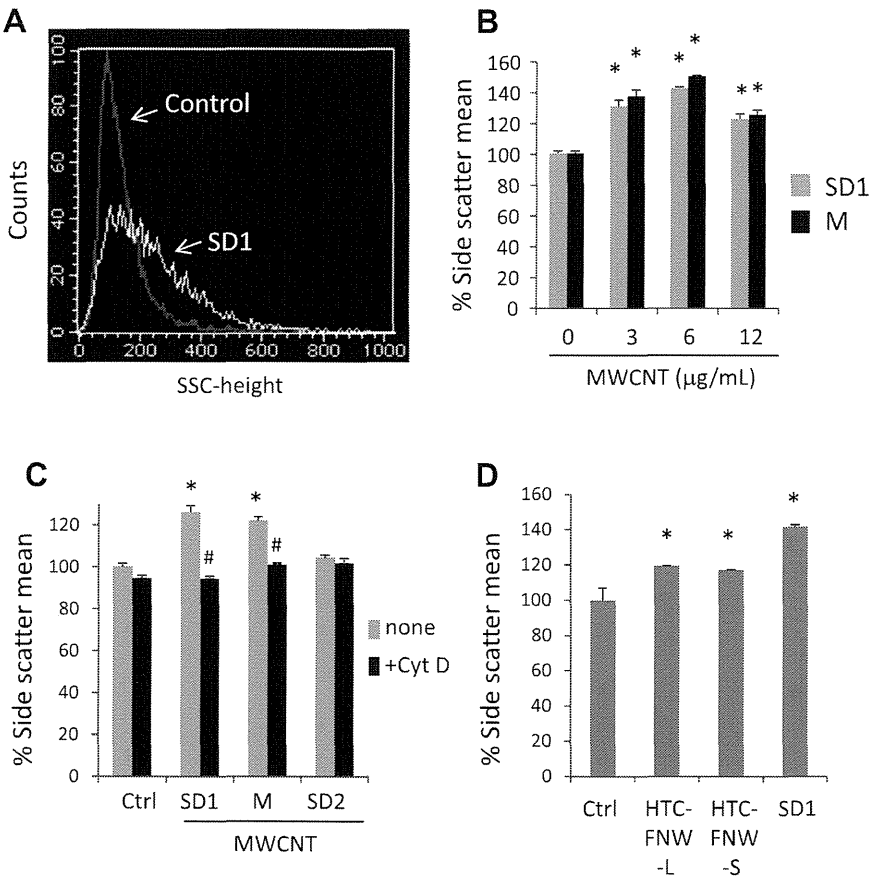

Fig. 2. Flow cytometry analysis shows cell internalization of MWCNTs and HTCFNWs. THP-1 cells were treated with or without cytochalasin D (0.2 μM) for 30 min and were then exposed to the indicated concentration of MWCNT-SD1, -SD2, -M, HTCFNW-L or -S dispersed in Tween 80 (final concentration, 0.002%) for 20 h. The cells were trypsinized and analyzed by flow cytometry. (A) Representative histogram shows the cell count vs side scatter (SSC) for cells treated without (gray line) or with MWCNT-SD1 (6 μg/mL) (white line). (B–D) Mean of the SSC value of cells treated without or with increasing concentrations of MWCNT-SD1 or -M (B), or 6 μg/mL of MWCNTs or HTCFNWs (C, D). Uptake was detectable as an increase in cell number with higher SSC. Data represent means ± S.D (n = 2 or 3). Significant difference from vehicle control (*) or between cytochalasin D-untreated and -treated cells (#).

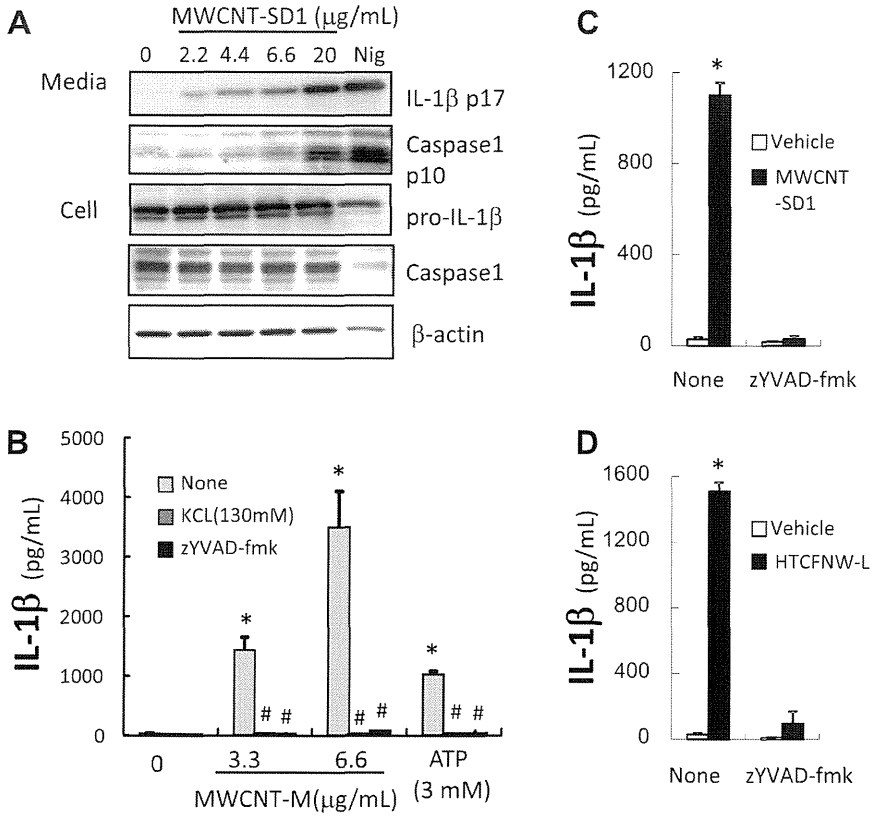

Fig. 3. MWCNT- and HTCFNW-induced IL-1β secretion accompanies caspase-1 cleavage and is repressed by extracellular KCl (130 mM) or a caspase-1 inhibitor. (A) THP-1 cells were stimulated for 6 h with the indicated amount (μg/mL of media) of MWCNT-SD1 dispersed in 0.002% Tween 20 or nigericin (Nig) (3.4 μM). The cell lysate and medium were analyzed by immunoblotting. (B–D) THP-1 cells were treated for 6 h with MWCNT-M or ATP (3 mM) (B), or MWCNT-SD1 (10 μg/mL) (C) and HTCFNW-L (10 μg/mL) (D) dispersed in 0.002% Tween 80 in the presence or absence of 130 mM KCl or the caspase-1 inhibitor zYVAD-fmk (10 μM). IL-1β in the medium was analyzed by the Milliplex immunoassay. Data represent means ± S.D ($n = 2$). Significant difference from vehicle control (*) or between inhibitor-untreated and -treated cells (#).

induce proinflammatory cytokine IL-1β production in human macrophage-like THP-1 cells (Fig. 1). Prominent IL-1β release by these nanomaterials was sensitive to the phagocytosis inhibitor cytochalasin D (Fig. 1B) and was accompanied by increases in cellular SSC values related to particle internalization (Fig. 2). Notably, HTCFNW-L and -S produced a potent and faint IL-1β release, respectively (Fig. 1C), whereas both fibers caused similar changes in the cellular SSC level (Fig. 2D). These findings clearly indicate that the needle-like shape and length of carbon nanofibers are critical to inducing IL-1β release after being taken up by cells.

The prominent IL-1β production by MWCNT-M, MWCNT-SD1, and HTCFNW-L was repressed by a high concentration of potassium or caspase-1 inhibitor and was accompanied by an increase in the active-form of caspase-1 release. Knockdown of NLRP3 by specific siRNAs diminished IL-1β production induced by these nanofibers, indicating that the NLRP3-containing inflammasome is involved in IL-1β release induced by fullerene-derived HTCFNW-L as well as long, needle-like MWCNTs.

NLRP3 is known to be activated by a variety of danger signals, including endogenous crystals of monosodium urate and cholesterol, exogenous silica crystals, aluminum salts, carbon nanotubes, and bacterial toxins, and the complex plays a critical role in IL-1β-mediated pathology [11,12]. Although the mechanism of NLRP3 activation is still unclear, potassium efflux, ROS generation, and lysosome destabilization have been implicated in NLRP3-inflammasome activation [11,12]. Changes in the redox environment have been suggested to modulate the NLRP3 inflammasome activation potential [27]. Our findings indicate that the ability of HTCFNW-L to induce NLRP3-mediated IL-1β release is comparable to that of MWCNT-M and -SD1. HTCFNWs have a needle-like morphology and similar size to MWCNT-M and -SD1. However, unlike MWCNTs, HTCFNWs contain no tubular structures or metal impurities such as Fe or Ni. Previous studies have suggested that metal contamination of CNTs is responsible for their toxicity [16–18] and cellular redox-response [19]. Importantly, HTCFNW-L and -S, which were synthesized from pure fullerene by liquid–liquid interfacial precipitation methods [23] followed by sintering with heat-treatment, contain no metal impurities. Thus, our findings clearly demonstrate that long, needle-like structures of MWCNTs and HTCFNW-L, but not metal contaminants, are required for NLRP3 inflammasome activation leading to the resulting IL-1β release.

The NLPR3-inflamasome has been implicated in several chronic inflammatory diseases such as metabolic syndrome, inflammatory bowel disease, atherosclerosis, and Alzheimer disease, as well as in regulating antimicrobial and mucosal immune responses [12,28]. Our findings raise concerns that MWCNTs may affect these diseases and responses through stimulating NLRP3-mediated IL-1β production.

In conclusion, we have shown for the first time that fullerene-derived HTCFNW-L as well as MWCNTs induces IL-1β release in an NLRP3-mediated process. Our findings indicate that the needle-like shape and length of MWCNTs, but not metal impurities or tubular structures, play a critical role in robust NLRP3 activation, which is closely implicated in chronic inflammatory diseases.

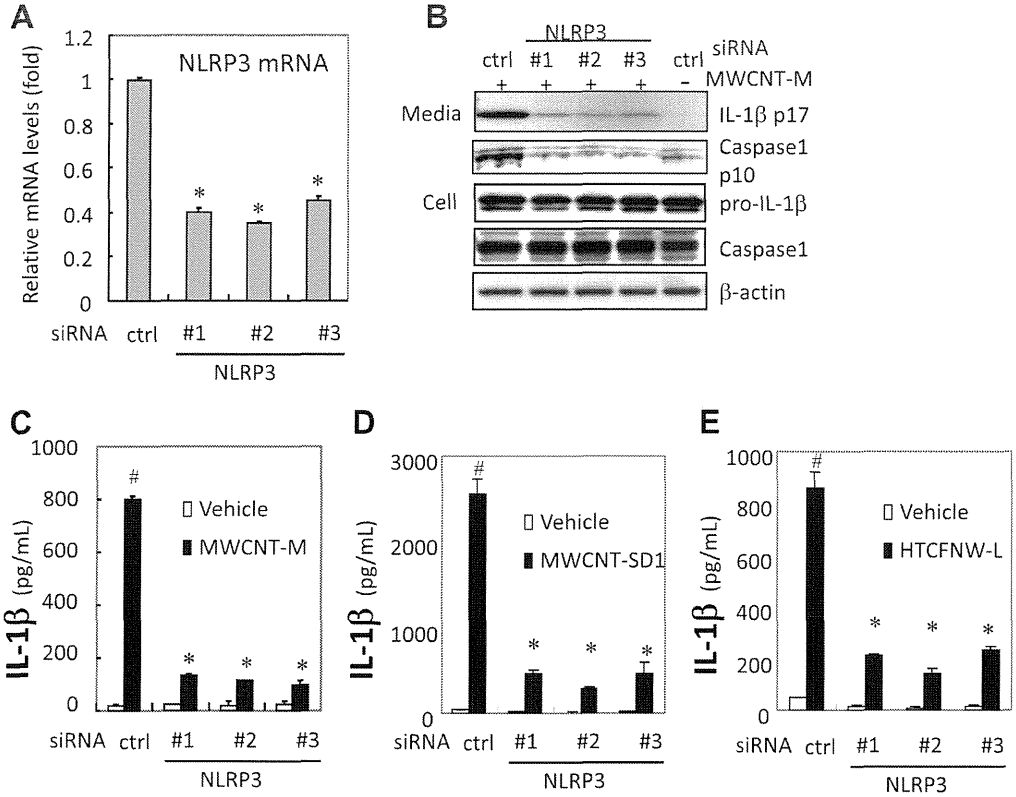

Fig. 4. Knockdown of NLRP3 diminishes MWCNT- and HTCFNW-elicited IL-1β secretion. THP-1 cells were transfected with either siRNA against three different sequences of NLRP3 (#1–3) or a negative control siRNA. After 24 h, cells were treated with MWCNT-M (6.6 μg/mL) (B, C), MWCNT-SD1 (10 μg/mL) (D) dispersed in 0.002% Tween 20, or HTCFNW-L (10 μg/mL) in Tween 80 (E) for 6 h. (A) NLRP3 mRNA levels were measured by quantitative real-time RT-PCR analysis normalized with the 18S rRNA. (B) IL-1β (p17) and caspase-1 (p10) in the medium and pro-IL-1β and caspase-1 in the cell lysate were analyzed by immunoblotting. (C–E) IL-1β in the medium was analyzed by the Milliplex immunoassay. Data represent means ± S.D. ($n = 3$ or 2). Significant difference from vehicle-treated control (#) or control siRNA-transfected cells (*).

Acknowledgments

This work was supported by a Health, Labor, and Welfare Sciences Research Grant (H21-kagaku-ippan-008, H24-kagaku-shitei-009, H26-kagaku-ippan-004), and in part by JSPS KAKENHI Grant Number 23590164.

References

[1] K. Donaldson, R. Aitken, L. Tran, V. Stone, R. Duffin, G. Forrest, A. Alexander, Carbon nanotubes: a review of their properties in relation to pulmonary toxicology and workplace safety, Toxicol. Sci. 92 (2006) 5–22.
[2] A. Takagi, A. Hirose, T. Nishimura, N. Fukumori, A. Ogata, N. Ohashi, S. Kitajima, J. Kanno, Induction of mesothelioma in p53+/- mouse by intraperitoneal application of multi-wall carbon nanotube, J. Toxicol. Sci. 33 (2008) 105–116.
[3] Y. Sakamoto, D. Nakae, N. Fukumori, K. Tayama, A. Maekawa, K. Imai, A. Hirose, T. Nishimura, N. Ohashi, A. Ogata, Induction of mesothelioma by a single intrascrotal administration of multi-wall carbon nanotube in intact male Fischer 344 rats, J. Toxicol. Sci. 34 (2009) 65–76.
[4] C.A. Poland, R. Duffin, I. Kinloch, A. Maynard, W.A. Wallace, A. Seaton, V. Stone, S. Brown, W. Macnee, K. Donaldson, Carbon nanotubes introduced into the abdominal cavity of mice show asbestos-like pathogenicity in a pilot study, Nat. Nanotechnol. 3 (2008) 423–428.
[5] A. Yamaguchi, T. Fujitani, K. Ohyama, D. Nakae, A. Hirose, T. Nishimura, A. Ogata, Effects of sustained stimulation with multi-wall carbon nanotubes on immune and inflammatory responses in mice, J. Toxicol. Sci. 37 (2012) 177–189.
[6] D.W. Porter, A.F. Hubbs, R.R. Mercer, N. Wu, M.G. Wolfarth, K. Sriram, S. Leonard, L. Battelli, D. Schwegler-Berry, S. Friend, M. Andrew, B.T. Chen, S. Tsuruoka, M. Endo, V. Castranova, Mouse pulmonary dose- and time course-responses induced by exposure to multi-walled carbon nanotubes, Toxicology 269 (2010) 136–147.
[7] P. Ravichandran, S. Baluchamy, R. Gopikrishnan, S. Biradar, V. Ramesh, V. Goornavar, R. Thomas, B.L. Wilson, R. Jeffers, J.C. Hall, G.T. Ramesh, Pulmonary biocompatibility assessment of inhaled single-wall and multiwall carbon nanotubes in BALB/c mice, J. Biol. Chem. 286 (2011) 29725–29733.
[8] J.P. Ryman-Rasmussen, M.F. Cesta, A.R. Brody, J.K. Shipley-Phillips, J.I. Everitt, E.W. Tewksbury, O.R. Moss, B.A. Wong, D.E. Dodd, M.E. Andersen, J.C. Bonner, Inhaled carbon nanotubes reach the subpleural tissue in mice, Nat. Nanotechnol. 4 (2009) 747–751.
[9] J. Xu, M. Futakuchi, H. Shimizu, D.B. Alexander, K. Yanagihara, K. Fukamachi, M. Suzui, J. Kanno, A. Hirose, A. Ogata, Y. Sakamoto, D. Nakae, T. Omori, H. Tsuda, Multi-walled carbon nanotubes translocate into the pleural cavity and induce visceral mesothelial proliferation in rats, Cancer Sci. 103 (2012) 2045–2050.
[10] E.J. Park, W.S. Cho, J. Jeong, J. Yi, K. Choi, K. Park, Pro-inflammatory and potential allergic responses resulting from B cell activation in mice treated with multi-walled carbon nanotubes by intratracheal instillation, Toxicology 259 (2009) 113–121.
[11] K. Schroder, J. Tschopp, The inflammasomes, Cell 140 (2010) 821–832.
[12] T. Strowig, J. Henao-Mejia, E. Elinav, R. Flavell, Inflammasomes in health and disease, Nature 481 (2012) 278–286.
[13] E. Meunier, A. Coste, D. Olagnier, H. Authier, L. Lefevre, C. Dardenne, J. Bernad, M. Beraud, E. Flahaut, B. Pipy, Double-walled carbon nanotubes trigger IL-1beta release in human monocytes through Nlrp3 inflammasome activation, Nanomedicine 8 (2012) 987–995.
[14] J. Palomaki, E. Valimaki, J. Sund, M. Vippola, P.A. Clausen, K.A. Jensen, K. Savolainen, S. Matikainen, H. Alenius, Long, needle-like carbon nanotubes and asbestos activate the NLRP3 inflammasome through a similar mechanism, ACS Nano 5 (2011) 6861–6870.
[15] H. Nagai, S. Toyokuni, Biopersistent fiber-induced inflammation and carcinogenesis: lessons learned from asbestos toward safety of fibrous nanomaterials, Arch. Biochem. Biophys. 502 (2010) 1–7.
[16] H. Haniu, Y. Matsuda, K. Takeuchi, Y.A. Kim, T. Hayashi, M. Endo, Proteomics-based safety evaluation of multi-walled carbon nanotubes, Toxicol. Appl. Pharmacol. 242 (2010) 256–262.
[17] M. Pacurari, X.J. Yin, J. Zhao, M. Ding, S.S. Leonard, D. Schwegler-Berry, B.S. Ducatman, D. Sbarra, M.D. Hoover, V. Castranova, V. Vallyathan, Raw single-wall carbon nanotubes induce oxidative stress and activate MAPKs, AP-1, NF-kappaB, and Akt in normal and malignant human mesothelial cells, Environ. Health Perspect. 116 (2008) 1211–1217.

[18] K. Pulskamp, S. Diabate, H.F. Krug, Carbon nanotubes show no sign of acute toxicity but induce intracellular reactive oxygen species in dependence on contaminants, Toxicol. Lett. 168 (2007) 58–74.
[19] V.E. Kagan, Y.Y. Tyurina, V.A. Tyurin, N.V. Konduru, A.I. Potapovich, A.N. Osipov, E.R. Kisin, D. Schwegler-Berry, R. Mercer, V. Castranova, A.A. Shvedova, Direct and indirect effects of single walled carbon nanotubes on RAW 264.7 macrophages: role of iron, Toxicol. Lett. 165 (2006) 88–100.
[20] C. Cheng, K.H. Muller, K.K. Koziol, J.N. Skepper, P.A. Midgley, M.E. Welland, A.E. Porter, Toxicity and imaging of multi-walled carbon nanotubes in human macrophage cells, Biomaterials 30 (2009) 4152–4160.
[21] R. Kato, K. Miyazawa, T. Nishimura, Z.M. Wang, High-resolution transmission electron microscopy of heat-treated C_{60} nanotubes, J. Phys: Conf. Ser. 159 (2009) 012024.
[22] K. Miyazawa, Synthesis and properties of fullerene nanowhiskers and fullerene nanotubes, J. Nanosci. Nanotechnol. 9 (2009) 41–50.
[23] K. Miyazawa, Y. Kuwasaki, A. Obayashi, M. Kuwabara, C_{60} nanowhiskers formed by the liquid–liquid interfacial precipitation method, J. Mater. Res. 17 (2002) 83–88.
[24] H. Nagai, Y. Okazaki, S.H. Chew, N. Misawa, Y. Yamashita, S. Akatsuka, T. Ishihara, K. Yamashita, Y. Yoshikawa, H. Yasui, L. Jiang, H. Ohara, T. Takahashi, G. Ichihara, K. Kostarelos, Y. Miyata, H. Shinohara, S. Toyokuni, Diameter and rigidity of multiwalled carbon nanotubes are critical factors in mesothelial injury and carcinogenesis, Proc. Natl. Acad. Sci. U.S.A. 108 (2011) E1330–E1338.
[25] P. Haberzettl, R. Duffin, U. Kramer, D. Hohr, R.P. Schins, P.J. Borm, C. Albrecht, Actin plays a crucial role in the phagocytosis and biological response to respirable quartz particles in macrophages, Arch. Toxicol. 81 (2007) 459–470.
[26] C. Dostert, V. Petrilli, B.R. Van, C. Steele, B.T. Mossman, J. Tschopp, Innate immune activation through Nalp3 inflammasome sensing of asbestos and silica, Science 320 (2008) 674–677.
[27] A. Rubartelli, Redox control of NLRP3 inflammasome activation in health and disease, J. Leukoc. Biol. 92 (2012) 951–958.
[28] M.T. Heneka, M.P. Kummer, A. Stutz, A. Delekate, S. Schwartz, A. Vieira-Saecker, A. Griep, D. Axt, A. Remus, T.C. Tzeng, E. Gelpi, A. Halle, M. Korte, E. Latz, D.T. Golenbock, NLRP3 is activated in Alzheimer's disease and contributes to pathology in APP/PS1 mice, Nature 493 (2013) 674–678.